Available online at www.sciencedirect.com
ScienceDirect
Journal of Solid State Chemistry 179 (2006) 3518–3524
JOURNAL OF SOLID STATE CHEMISTRY
www.elsevier.com/locate/jssc

Structural and compositional variations in Ta_3N_5 produced by high-temperature ammonolysis of tantalum oxide

Stuart J. Henderson, Andrew L. Hector*

School of Chemistry, University of Southampton, Highfield, Southampton SO17 1BJ, UK

Received 21 March 2006; received in revised form 19 June 2006; accepted 14 July 2006
Available online 21 July 2006

Abstract

A series of samples of Ta_3N_5 (*Cmcm*, $a = 3.89$ Å, $b = 10.22$ Å, $c = 10.28$ Å) have been produced by high-temperature ammonolysis of amorphous tantalum oxide under various temperature and heating time regimes. These were characterised by powder diffraction (X-ray and neutron), combustion microanalysis, thermogravimetric analysis and transmission electron microscopy. All samples were found to contain oxide in the 3-coordinate anion site and the *b*-axis length was sensitive to compositional variation. Samples heated for longer times at higher temperatures were anion deficient. The compositions of the samples have been related to their optical band gap UV–visible spectra. This work highlights the importance of careful compositional analysis when samples of nitride materials are produced for real-world applications.

Keywords: Tantalum nitride; Non-stoichiometry; Oxide; Powder neutron diffraction; Band gap

1. Introduction

Tantalum (V) nitride has an optical band gap of 2.08 eV [1], making it a useful red pigment [2]. Pearlescent effect pigments can be produced by coating silica flakes with Ta_3N_5 using fluidized bed apparatus [3]. The compound has been shown to be an active photocatalyst in the visible region of the electromagnetic spectrum, including a quantum efficiency of ca. 10% for overall water splitting and good hydrolytic stability [4]. Inverse opal thin films of Ta_3N_5 show promise as optical wavelength photonic structures [5], it has also been investigated for use as a capacitor dielectric [6], a gas-sensor material for propanal [7] and an antireflective coating in photolithography [8].

Ta_3N_5 is composed of irregular TaN_6 octahedra with both three and four coordinate nitrogen atoms and has the pseudobrookite (Fe_2TiO_5) structure, Fig. 1. The structure was confirmed [9] using powder neutron diffraction (PND) on samples prepared by ammonolysis of $TaCl_5$, this route was originally reported by Moureu and Hamblet [10]. However, some diffraction studies on Ta_3N_5 have been based on material derived from the reaction of Ta_2O_5 with ammonia [11] and this is a common preparative method in the more recent application-based studies [1–5,7]. While elemental analysis has been undertaken in these investigations, some oxide is always found and the nitride content fails to reach that of stoichiometric Ta_3N_5 [4,12–15]. Often this is attributed to air oxidation causing an unrepresentative result in surface-based methods or to combustion analysis giving a low nitrogen content on a refractory material. Hara et al. [15] nitrided a Ta_2O_5 film at 850 °C in the X-ray photoelectron spectrometer antichamber with various flow rates and reaction times. Even under these conditions, with no air exposure, the surface composition did not become richer in nitrogen than $Ta_3N_{4.8}O_{0.3}$. Questions therefore remain about whether residual oxide is located only on the surface or also in the bulk of the material.

The band gap of a material can be varied by altering the electronegativity difference between the cationic and anionic elements [16]. Nitrogen has a lower electronegativity than oxygen and the presence of O^{2-} in the anionic framework will act to increase the band gap, altering the

*Corresponding author. Fax: +44 2380596805.
E-mail address: a.l.hector@soton.ac.uk (A.L. Hector).

0022-4596/$ - see front matter © 2006 Elsevier Inc. All rights reserved.
doi:10.1016/j.jssc.2006.07.021

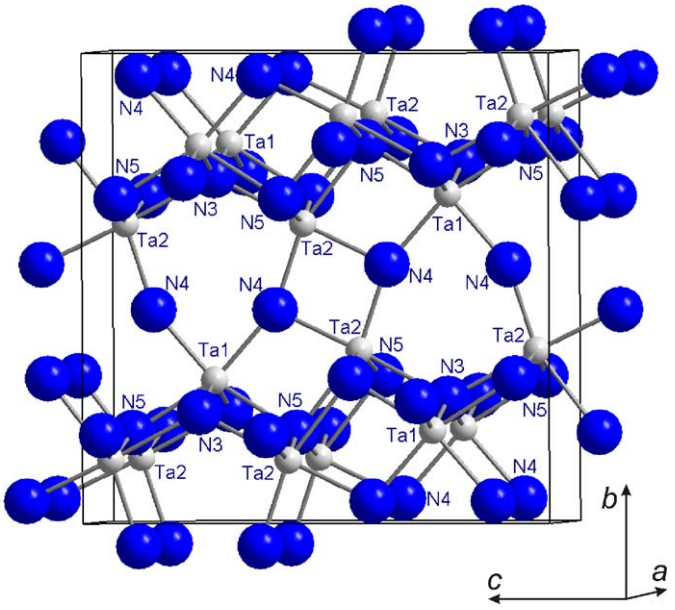

Fig. 1. The unit cell of Ta_3N_5 showing 6-coordinate Ta^{5+} and 3- and 4-coordinate N^{3-} sites.

compound's optical properties. Thus Ta_3N_5 is red ($E_g = 2.08$ eV) whereas TaON is yellow (2.5 eV). Electronic structure calculations for Ta_3N_5 predict a smaller band gap than that observed experimentally [1]. Low band gap values from density functional theory are common, but some oxide content in the measured materials could also contribute to this deficiency.

Other aspects of the synthesis of Ta_3N_5 from Ta_2O_5 are intriguing; for example, at 850 °C this route can lead to porous crystallites [17] and the resulting increase in surface area may improve the catalytic properties. The colour and catalytic properties of materials are also dependent on crystallite size and morphology as well as the surface composition and band gap. Many properties are likely to depend on an interplay between the composition (harsher conditions resulting in higher nitrogen content and smaller band gap) and microstructure (harsher conditions closing up pores and annealing particles).

In view of the many applications envisaged for oxide-derived Ta_3N_5, a re-evaluation of how its composition, structure and properties vary with the synthesis conditions is timely. Of particular interest is the oxide content and its location within the Ta_3N_5 lattice. PND is useful in distinguishing oxide ($B_{coh} = 5.80$ fm) from nitride (9.36 fm), and here is used in conjunction with thermogravimetric analysis and combustion microanalysis to obtain a detailed compositional information. The analysis of PND peak shape can also give useful information about the sample morphology and these results are combined with transmission electron microscopy (TEM). Finally, UV–visible spectra are used to examine the effect of the synthesis conditions on the optical properties.

2. Experimental section

The amorphous tantalum oxide precursor was prepared from rapidly hydrolysed tantalum ethoxide prepared via a modification of a published route [18]. $TaCl_5$ (40 g) was stirred with ethanol (400 ml) under flowing ammonia gas for 2 h to form $Ta(OEt)_5$ and NH_4Cl. The mixture was poured into dilute aqueous ammonia (1 L, ~2 mol dm^{-3}). The white precipitate was collected by filtration, washed with water and dried at 100 °C. The loosely powdered precursor (~1 g) was placed in an alumina boat inside a silica furnace tube and nitrided under flowing ammonia gas (Air Products, anhydrous with <200 ppm H_2O) with a flow rate of 2 L min^{-1} at a series of temperatures (680, 700, 750, 800 and 900 °C—tube furnace with ca. 15 cm hot zone) and times (2, 4, 8, 24 and 120 h). The products studied by PND were visually homogeneous when removed from the furnace, though some of the samples heated for shorter times had a colour gradient, with the end closest to the ammonia supply apparently most nitrided.

Samples were characterised by powder X-ray diffraction using a Bruker D8 diffractometer with Cu$K_{\alpha 1}$ radiation. Phases present were identified by comparison with the PDF2 database [19]. Thermogravimetric analyses were carried out on a Mettler Toledo TGA/SDTA851e under flowing oxygen from 25 to 1000 °C, complete decomposition to Ta_2O_5 occurs at around 700 °C. TEM was performed on a Jeol JEM-3010 microscope at 300 kV accelerating voltage, samples were prepared by ultrasound dispersal in toluene followed by deposition on carbon-coated grids. Diffuse reflectance UV–visible spectra were obtained using a Perkin Elmer Lambda 35 spectrometer with an integrating sphere in the range 380–780 nm.

PND data were collected at ambient temperature in 6-mm vanadium cans using the medium resolution, high-intensity time-of-flight POLARIS diffractometer at the ISIS facility. Data from the backscattered bank ($2\theta = 145°$) with a time-of-flight range of 2–19 μs ($d = 0.324-3.084$ Å, 3993 reflections) were used for structural refinement with the GSAS [20] suite of programs. Scale factor, lattice parameters and 10 background terms in a cosine Fourier series (GSAS function no. 2) were refined, followed by a linear absorption correction, atom positions, isotropic temperature factors and peak shape (GSAS profile type 3). Finally anisotropic temperature factors were used and the anion sites were refined as mixed O/N, with total occupancy fixed at 1, these sites were set as nitrogen if a small negative or zero O occupancy resulted. Crystallite size and strain information were obtained using the method described in the GSAS manual [21], see Supplementary information for more details.

3. Results and discussion

Ta_3N_5 is red in colour, so visual impression is a good indication of its phase purity. Sample colours and the phases observed by PXD are shown in Table 1 and the

Table 1
Colour and PXD phase identification with various heating times and temperatures

	680 °C	700 °C	750 °C	800 °C	900 °C
2 h	Yellow, amorphous	Yellow-brown, amorphous	Orange-brown, Ta_3N_5 plus amorphous	Orange, Ta_3N_5 plus TaON	Orange-red, Ta_3N_5 plus TaON
4 h	Yellow-brown, amorphous	Brown, amorphous	Orange-brown, Ta_3N_5 plus a little amorphous	Orange-red, Ta_3N_5 plus TaON	Red, Ta_3N_5 plus TaON
8 h	Brown, Ta_3N_5 plus amorphous	Orange-brown, Ta_3N_5 plus a little amorphous	Orange-red, Ta_3N_5	Red, Ta_3N_5	Red, Ta_3N_5
24 h	Orange-red, Ta_3N_5	Red, Ta_3N_5	Red, Ta_3N_5	Red, Ta_3N_5	Red, Ta_3N_5
120 h	Red, Ta_3N_5	Red, Ta_3N_5	Red, Ta_3N_5	Red, Ta_3N_5	Red, Ta_3N_5

UV–visible spectra of samples fired for 8 h are shown in Fig. 2. Generally, samples which have an orange or brown colouration contain amorphous material or TaON. This was determined by PXD and Fig. 3 shows typical patterns for crystalline and amorphous samples. All samples heated for 2 or 4 h were impure with the sample size used, hence the work focused on samples heated for 8 h or longer. With smaller sample sizes (~100 mg) than we needed for the PND studies, apparently phase pure Ta_3N_5 can be obtained in much shorter time periods.

The composition of samples, Table 2, was obtained using a combination of combustion microanalysis (% C, H, N) and TGA (% Ta). Oxygen content was inferred by difference. Carbon and hydrogen content was typically 0.1% or less except in the sample annealed at 680 °C for 8 h, where 0.24% H was found. The general trend is for nitrogen content to increase and oxygen to decrease with increasing synthesis temperature or time. Samples made at 680 °C were found to be anion rich, from $Ta_3N_{3.99}O_{3.36}$ after 8 h (though amorphous material was observed in the PXD and H was found in the microanalysis) to $Ta_3N_{4.76}O_{0.56}$ after 120 h. Samples were not found to be oxide free even after heating at 900 °C, where the composition was $Ta_3N_{4.76}O_{0.25}$ after 8 h, $Ta_3N_{4.73}O_{0.21}$ after 24 h and $Ta_3N_{4.67}O_{0.23}$ after 120 h. Anion deficient samples were obtained after 24 h at 900 °C and after 120 h at 800 or 900 °C. Note that at 900 °C, the nitrogen content was reduced with longer heating time, at all other temperatures the nitrogen content increased with heating time. In nitrogen, Ta_3N_5 starts to lose mass and decompose to TaN at around 800 °C, a single step weight loss is complete by 1000 °C (TGA). The ammonia atmosphere has stabilised the Ta_3N_5 phase to 900 °C but the reducing N content shows that it is close to its decomposition temperature.

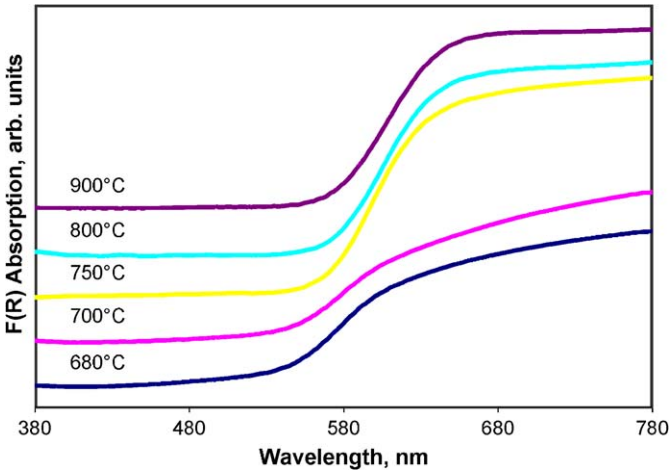

Fig. 2. UV–visible spectra for samples heated for 8 h at various temperatures.

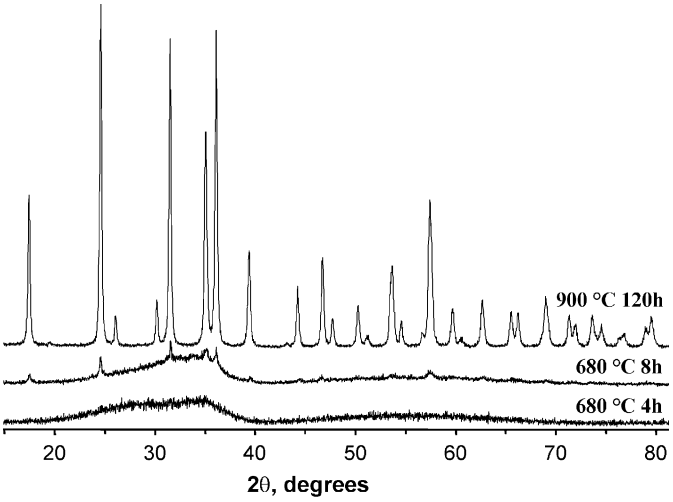

Fig. 3. PXD patterns of samples showing crystalline Ta_3N_5, a crystalline-amorphous mixture and amorphous material.

3.1. Neutron diffraction data

PND data were collected in order to refine the anion occupations and yield compositional information on the crystalline Ta_3N_5 material directly. This is complementary to the analytical data, which gives the composition of the material as a whole and can be affected by amorphous material or differences at particle surfaces. The structure of Ta_3N_5 consists of irregular TaN_6 octahedra sharing edges

Table 2
Variation in composition of Ta_3N_5 samples with preparation conditions as obtained by (top) microanalysis and TGA or by (bottom) PND

	680 °C	700 °C	750 °C	800 °C	900 °C
8 h	$Ta_3N_{3.99}O_{3.36}$	$Ta_3N_{4.28}O_{1.68}$	$Ta_3N_{4.62}O_{0.64}$	$Ta_3N_{4.61}O_{0.51}$	$Ta_3N_{4.76}O_{0.25}$
	—	$Ta_3N_{4.43}O_{0.57}$	$Ta_3N_{4.63}O_{0.37}$	$Ta_3N_{4.68}O_{0.32}$	$Ta_3N_{4.77}O_{0.23}$
24 h	$Ta_3N_{4.59}O_{0.96}$	$Ta_3N_{4.67}O_{0.74}$	$Ta_3N_{4.68}O_{0.38}$	$Ta_3N_{4.72}O_{0.40}$	$Ta_3N_{4.73}O_{0.21}$
	$Ta_3N_{4.56}O_{0.44}$	$Ta_3N_{4.66}O_{0.34}$	$Ta_3N_{4.68}O_{0.32}$	$Ta_3N_{4.67}O_{0.33}$	$Ta_3N_{4.74}O_{0.26}$
120 h	$Ta_3N_{4.76}O_{0.56}$	$Ta_3N_{4.75}O_{0.61}$	$Ta_3N_{4.85}O_{0.27}$	$Ta_3N_{4.80}O_{0.13}$	$Ta_3N_{4.67}O_{0.23}$
	$Ta_3N_{4.71}O_{0.29}$	$Ta_3N_{4.65}O_{0.35}$	$Ta_3N_{4.71}O_{0.29}$	$Ta_3N_{4.78}O_{0.22}$	$Ta_3N_{4.80}O_{0.20}$

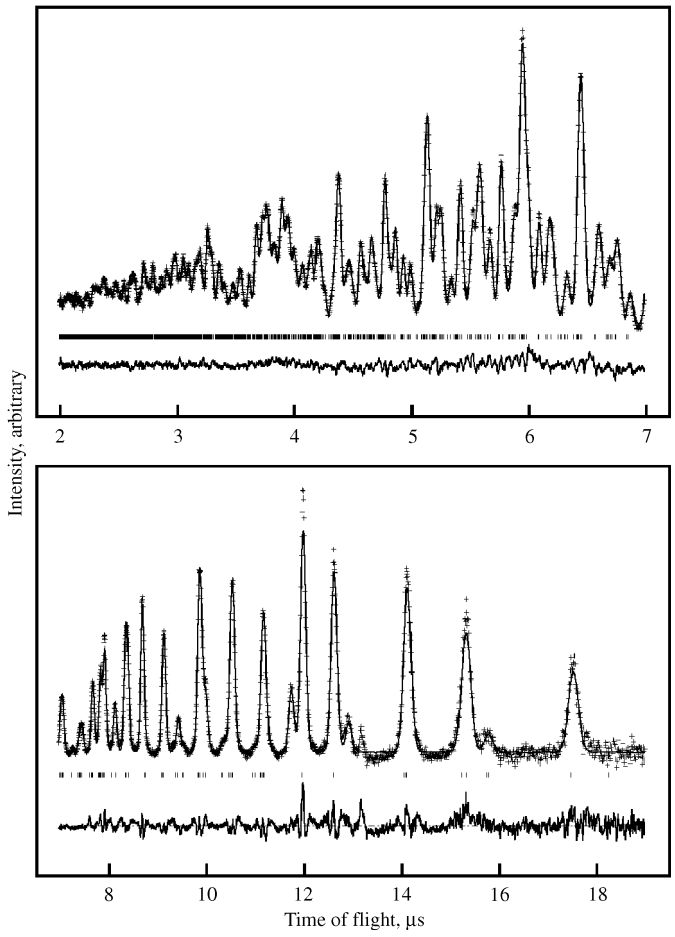

Fig. 4. Fit to the PND pattern of Ta_3N_5 produced at 750 °C with a heating time of 24 h. Crosses mark the data points, upper continuous line the calculated profile and lower continuous line the difference, tick marks are the positions of allowed reflections. The unfitted peak at 12.8 μs is due to the vanadium sample can.

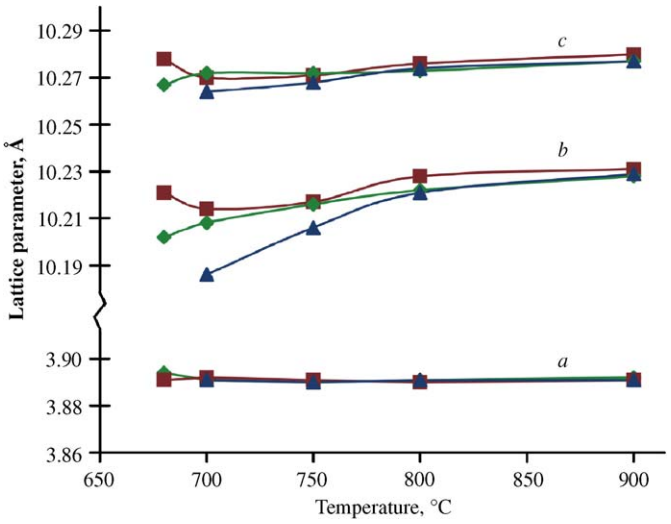

Fig. 5. Variation of lattice parameters of Ta_3N_5 with synthesis conditions. Squares indicate samples heated for 120 h, diamonds for 24 h and triangles for 8 h.

and corners, Fig. 1. Of particular interest here are the anion sites, of which there are three, N(3) and N(5) are 4-coordinate whereas N(4) is 3-coordinate.

Initial refinements with a stoichiometric Ta_3N_5 model yielded reasonable fits, though with slightly high extracted thermal displacement parameters on N(3) and N(4). Use of anisotropic thermal displacement parameters and mixed occupancy (O, N) on these sites yielded much improved fits, typically with $R_{wp}<2\%$ and $R_p<4\%$. The O content of the N(5) site refined to a slightly negative value (within e.s.d. of zero), indicating full occupancy with N, and was set at zero. This was sometimes also true of N(3). The 3-coordinate N(4) site was always, however, refined to a noteworthy oxide content. A typical fit is shown in Fig. 4 and the lattice parameters in Fig. 5. Only a small variation is observed between samples in *a* or *c*, whereas *b* is much more sensitive to heating time and temperature. The structure of Ta_3N_5 can be considered a double layer of Ta atoms linked by N(3) and N(5), with N(4) joining these layers, Fig. 1. Hence it is unsurprising that variations in the N(4) composition (oxygen substitution or reduced occupancy) are more easily accommodated within this structure than variations on the other N sites. Any changes to the composition of the N(4) site will also affect the *b*-axis length more than *a* or *c* because the layers stack in this direction (and the ionic radius of O^{2-} is around 0.08 Å shorter than that of N^{3-} [22]). Interestingly the previous PND study of the Ta_3N_5 structure [9] reported a high thermal displacement parameter for N(4) but this was not discussed.

The compositions of samples derived by PND as described above are shown in Table 2. Any anion site could be occupied by N, O or a vacancy whereas PND can only gauge the total scattering from the site and cannot deconvolute these three parameters. Hence, the sites were assumed to be fully occupied with the scattering described by

$$\text{Scattering} = (9.36 \times \text{N occupancy}) + (5.80 \times (1 - \text{N occupancy})).$$

A more accurate description would be

$$\text{Scattering} = (9.36 \times \text{N occupancy}) + (5.80 \times \text{O occupancy}) + (0 \times \text{N occupancy}),$$

where 9.36 and 5.80 are the coherent scattering lengths in fm of N and O, respectively. Comparison of the analytical and PND-derived compositions in Table 2 reveals three scenarios:

(1) In samples heated at 700 °C and below, also those heated for 8 h at 750 and 800 °C, the O-content in the analysis is markedly higher than that from the PND data. This can be attributed either to some amorphous oxide or oxide nitride, or to a crystalline but anion-rich/cation-deficient Ta_3N_5-type phase. In the latter case, the stoichiometric model employed in the PND refinements would result in a low modelled anion content, which would be compensated by an increase in the proportion of the stronger:weaker anion content, i.e. the proportion of N:O suggested by the PND would be too high. The lack of diffraction evidence for amorphous material combined with the varying lattice parameters would suggest that the latter explanation applies to most of these samples. It would seem likely that both scenarios apply to the samples heated for 8 h at 680 and 700 °C, where amorphous material was observed by PXD. The anion-rich materials may contain –OH, $–NH_2$ or >NH groups (hence the analysed H content in one sample), this is necessary to maintain charge balance with the analysed stoichiometries.
(2) The samples in the shaded region of Table 2 have similar analytical and PND compositions, suggesting roughly stoichiometric materials. Note that in all cases the oxide content is significant.
(3) Samples heated for 24 h at 900 °C or for 120 h at 800 or 900 °C were found to be anion deficient, this is consistent with the observation that Ta_3N_5 starts to lose mass at around 800 °C in flowing N_2. In these samples the proportion of N:O would be underestimated by PND. However, the analysis still shows that oxide is present to a significant extent.

Clearly some correlation will exist between the anion fractional occupancies obtained from PND and the thermal displacement parameters. However, the data contained a large number of diffraction peaks and the refinements were stable, thus the statistical errors (see Supplementary Information) on these parameters were small enough to conclude that the effects described above are real.

PND peak shape analysis shows that for a given annealing time, crystallite size stays relatively constant up to 800 °C, Fig. 6, before increasing more rapidly between 800 and 900 °C as diffusion becomes more significant. Strain decreases steadily with annealing time and temperature as the samples crystallise and the composition becomes more homogeneous. A small decrease in the crystallite size is observed between 680 and 750 °C in the samples annealed for 24 h. TEM, Fig. 7, shows that porous, quite complex, single-crystalline shapes are present at 680 °C, these complex shapes are larger than the PND crystallite size would suggest. By 800 °C these have annealed into more rounded, solid crystallites with similar size to that suggested from PND. It appears that the sintering process is mainly intraparticular up until 800 °C with crystallites

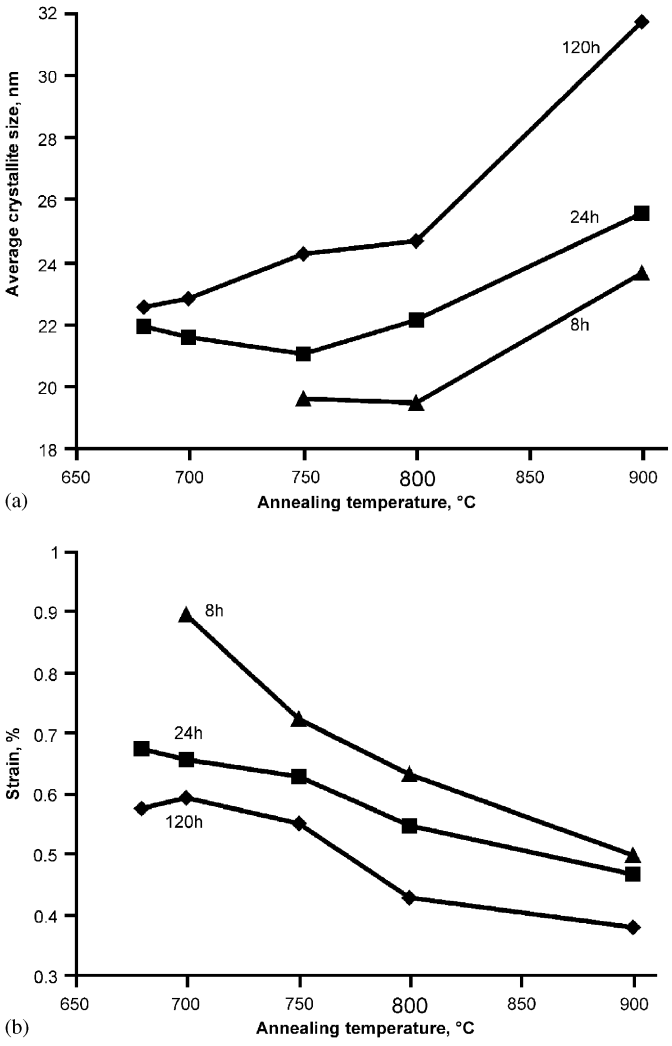

Fig. 6. Variation in crystallite size and strain obtained by analysis of the PND peak shape.

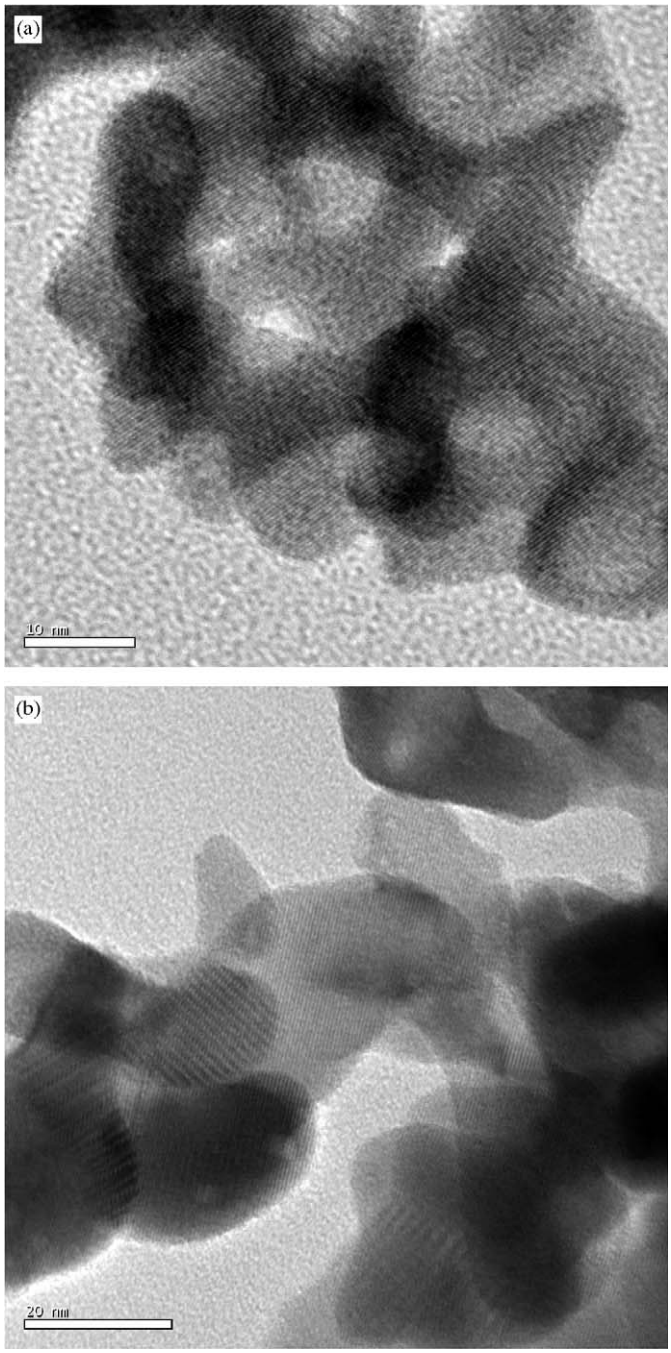

Fig. 7. Transmission electron micrographs of samples fired for 24 h at 680 °C (left) and 800 °C (right).

losing porosity and reductions thus being observed in the PND correlation lengths, then interparticle reactions begin to occur to a significant extent.

3.2. Effect of composition on optical properties

UV–visible spectra show a step in the absorbance at around 600 nm, corresponding to the band gap of Ta_3N_5. Optical band gap data for samples produced in this study are shown in Fig. 8. Generally the band gap decreases with

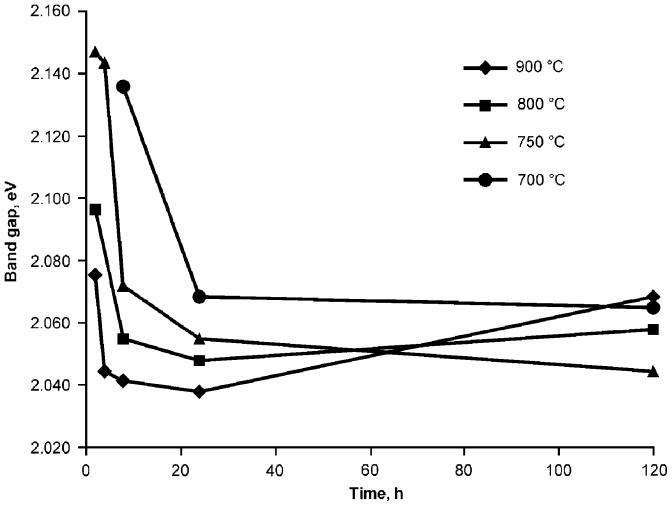

Fig. 8. Variation of optical band gap with synthesis conditions.

increasing nitrogen content and as the anion surplus and oxygen content fall. This is as expected—nitrogen is less electronegative and the valence band should be at higher energy with greater N content. The E_g values obtained herein are slightly lower for most samples than the published [1] value of 2.08 eV. It is noteworthy that the samples heated at 800 and 900 °C for 120 h have a larger bandgap than those heated at the same temperatures for 24 h. These samples are anion deficient and some reduction in the population of the valence band could be responsible for this effect. These results show the sensitivity of the behaviour of this phase to oxide content and to non-stoichiometry, and hence demonstrates the need to fully analyse the composition of Ta_3N_5 samples proposed for real-world applications.

4. Conclusions

Significant amounts of oxide ions remain in Ta_3N_5 samples prepared by ammonolysis of Ta_2O_5, even after extended heating periods in anhydrous NH_3. This oxide is located in the three-coordinate anion site in the Ta_3N_5 structure. The optical band gap and lattice parameters of Ta_3N_5 are affected by the oxide content—the *b*-axis length is found to be particularly sensitive due to the position of the three coordinate nitrogen site within the structure. At higher temperatures, the Ta_3N_5 structure becomes anion deficient and this results in an increase in the optical band gap.

Acknowledgments

The authors thank the Royal Society for support through a University Research Fellowship (ALH), EPSRC for a studentship (SJH), CCLRC for beam time at ISIS on Grant RB20250, Dr. R.I. Smith for assistance with PND data collection and Dr. B.A. Cressey for collecting the TEM data.

Appendix A. Supplementary materials

Supplementary data associated with this article can be found in the online version at doi:10.1016/j.jssc.2006.07.021.

References

[1] C.M. Fang, E. Orhan, G.A. de Wijs, H.T. Hintzen, R.A. de Groot, R. Marchand, J.Y. Saillard, G.J. de With, J. Mater. Chem. 11 (2001) 1248.

[2] M. Jansen, E. Guenther, H.P. Letschert, German Patent 199 07 618.9, 1999.

[3] S. Bertaux, P. Reynders, J.M. Heintz, M. Lerch, Mater. Sci. Eng. B 121 (2005) 137.

[4] (a) G. Hitoki, A. Ishikawa, T. Takata, J.N. Kondo, M. Hara, K. Domen, Chem. Lett. 7 (2002) 736;
(b) M. Hara, G. Hitoki, T. Takata, J.N. Kondo, H. Kobayashi, K. Domen, Catal. Today 78 (2003) 555.

[5] A. Rugge, J.S. Park, R.G. Gordon, S.H. Tolbert, J. Phys. Chem. B 109 (2005) 3764.

[6] K.J. Lee, H.S. Yang, Japanese Patent 2001237399, 2001.

[7] O. Merdrignac-Conanec, M. Kerlau, M. Guilloux-Viry, R. Marchand, N. Barsan, U. Weimar, Silic. Ind. 69 (2004) 141.

[8] A. Jain, K. Lucas, US Patent 5741626, 1998.

[9] N.E. Brese, F.J. Disalvo, M. O'Keeffe, P. Rauch, Acta Crystallogr. C 47 (1991) 2291 and see references therein for the original structure determinations and discussion of a possible lower symmetry structure.

[10] H. Moureu, C.H. Hamblett, J. Am. Chem. Soc. 59 (1937) 33.

[11] G. Brauer, J.R. Weidlein, Angew. Chem. 77 (1965) 218.

[12] Q. Zhang, L. Gao, Langmuir 20 (2004) 9821.

[13] V.G. Brauer, J. Weidlein, J. Strähle, Z. Anorg. Allg. Chem. 348 (1966) 298.

[14] J.H. Swisher, M.H. Read, Metall. Trans. 3 (1972) 489.

[15] M. Hara, E. Chiba, A. Ishikawa, T. Takata, J.N. Kondo, K. Domen, J. Phys. Chem. B 107 (2003) 13441.

[16] E. Günther, M. Jansen, Mater. Res. Bull. 36 (2001) 1399.

[17] D. Lu, G. Hitoki, E. Katou, J.N. Kondo, M. Hara, K. Domen, Chem. Mater. 16 (2004) 1603.

[18] A.A. Melas, European Patent EP0251432, 07/01/1988.

[19] Powder Diffraction File, Version 2.4, International Centre for Diffraction Data, Swarthmore, PA 19073, USA, 2004.

[20] Generalized structure analysis system, R.B. Von Dreele, A.C. Larson, Los Alamos National Laboratory, NM87545, USA, December 2002 release.

[21] A.C. Larson, R.B. Von Dreele, GSAS Manual, LANSCE MS-H805, Los Alamos National Laboratory, Los Alamos NM, NM 87545, 2000.

[22] R.D. Shannon, Acta Crystallogr., Sect. A 32 (1976) 751.